Mathematical Sciences Letters
An International Journal

http://dx.doi.org/10.12785/msl/040205

Comparative Studies for Different Image Restoration Methods

N. H. Sweilam[1,*], *A. M. Nagy*[2,*], *T. H. Farag*[1] *and A. S. Abo-Elyazed*[1]

[1] Department of Mathematics, Faculty of Science, Cairo University, Giza, Egypt
[2] Department of Mathematics, Faculty of Science, Benha University, Egypt

Received: 29 Nov. 2014, Revised: 3 Feb. 2015, Accepted: 9 Feb. 2015
Published online: 1 May 2015

Abstract: Image restoration refers to the problem of removal or reduction of degradation in blurred noisy images. The image degradation is usually modeled by a linear blur and an additive white noise process. The linear blur involved is always an ill-conditioned which makes image restoration problem an ill-posed problem for which the solutions are unstable. Procedures adopted to stabilize the inversion of ill-posed problem are called regularization, so the selection of regularization parameter is very important to the effect of image restoration. In this paper, we study some numerical techniques for solving this ill-posed problem. Dynamical systems method (DSM), Tikhonov regularization method, L-curve method and generalized cross validation (GCV) are presented for solving this ill-posed problems. Some test examples and comparative study are presented. From the numerical results it is clear that DSM showed improved restored images compared to L-curve and GCV.

Keywords: Dynamical systems method; Tikhonov regularization method; L-curve method; GCV method; Image restoration

1 Introduction

Image restoration is the process of removing blur and noise from degraded images to recover an approximation of the original image. This field of imaging technology is becoming increasingly important in many scientific applications such as astronomy, medical imaging, military, surveillance, iris scanning, microscopy and video communication technologies ([1], [4], [16], [18]). The degradation consists of two distinct processes: the deterministic blur and the random noise. The blur may be due to a number of reasons, such as motion, defocusing, and atmospheric turbulence. The noise may originate in the image formation process, the transmission process, or a combination of them. Many image restoration algorithms have their roots in well-developed theory, the solution of ill-posed problem, linear algebra and numerical analysis ([3], [14], [17]).

The image degradation process can be modeled by a linear blur and an additive noise process, that is

$$b = Ax + n, \tag{1}$$

where b, x, n are $MN \times 1$ vectors and represent respectively the lexicographically ordered $M \times N$ pixel observed degraded image, original image, and additive noise. The matrix A represents the degradation matrix of size $MN \times MN$, which may represent a spatially invariant or a spatially varying degradation [25]. The image restoration problem is an inverse procedure to obtain an approximation of the original image x based on the image degradation model. It is an ill-posed problem, which means that a small perturbation in the data leads to a large perturbation in the solution. Therefore, a regularization is needed to avoid computing solutions that are corrupted by noise. One of the most popular regularization techniques is Tikhonov regularization which was first proposed and studied extensively in the 1960's and 1970's ([23], [24]), based on the minimization

$$\min_x \{\|Ax - b\|_2^2 + \alpha \|Lx\|_2^2\},$$

where $\alpha > 0$ is a constant, called a regularization parameter and the matrix L is called regularization matrix and it is typically either the identity matrix or a discrete approximation to a derivative operator, such as the Laplacian. The Tikhonov regularization in standard form when $L = I$ is given as follows

$$\min_x \{\|Ax - b\|_2^2 + \alpha \|x\|_2^2\}. \tag{2}$$

* Corresponding author e-mail: n_sweilam@yahoo.com, abdelhameed_nagy@yahoo.com

© 2015 NSP
Natural Sciences Publishing Cor.

Then it follows immediately that the Tikhonov problem can be reformulated as

$$x_\alpha = (A^TA+\alpha I)^{-1}A^Tb. \quad (3)$$

By solving the linear least squares problem using the singular value decomposition (SVD) of A, we obtain

$$x_\alpha = \sum_{i=1}^{n}\left(\frac{\sigma_i^2}{\sigma_i^2+\alpha}\right)\frac{u_i^Tb}{\sigma_i}v_i, \quad (4)$$

where the numbers σ_i are called the singular values of A, and the vectors u_i and v_i are referred to as the left and right singular vectors of A, respectively.

The determination of the regularization parameter α, is crucial and is still under intensive research. In this paper, we use the L-curve method, generalized cross validation (GCV) method and Dynamical systems method (DSM) to choose a good regularization parameter.

2 L-Curve Method

The L-curve method is proposed by Lawson and Hanson [15], later Hansen in ([7], [10]) used it as a parameter-choice method. The L-curve is a log-log plot of the norm of a regularized solution $\|Lx\|_2$ versus the residual norm $\|Ax-b\|_2$ and its names comes from the characteristic shape of the curve. The best regularization parameters α should lie in the corner of the L-curve.
The curvature of the L-curve plays an important role in the understanding and use of the L-curve. We will derive a convenient expression for this curvature [9]. Let $\alpha > 0$,

$$\eta_\alpha = \|x_\alpha\|_2^2, \qquad \rho_\alpha = \|Ax_\alpha - b\|_2^2, \quad (5)$$

and

$$\hat{\eta}_\alpha = \log\eta_\alpha, \qquad \hat{\rho}_\alpha = \log\rho_\alpha; \quad (6)$$

such that the L-curve is a plot of $\hat{\eta_\alpha}/2$ versus $\hat{\rho_\alpha}/2$, then the curvature κ of the L-curve, as a function of α, is given by:

$$\kappa_\alpha = 2\frac{\hat{\rho}'_\alpha\hat{\eta}''_\alpha - \hat{\rho}''_\alpha\hat{\eta}'_\alpha}{((\hat{\rho}'_\alpha)^2+(\hat{\eta}'_\alpha)^2)^{3/2}}, \quad (7)$$

where $\hat{\eta}'_\alpha$, $\hat{\rho}'_\alpha$, $\hat{\eta}''_\alpha$, and $\hat{\rho}''_\alpha$ denote the first and second derivatives of $\hat{\eta}_\alpha$ and $\hat{\rho}_\alpha$ with respect to α.
The first derivatives of $\hat{\eta}_\alpha$ and $\hat{\rho}_\alpha$ with respect to α is given by:

$$\hat{\eta}'_\alpha = \frac{\eta'_\alpha}{\eta_\alpha}, \qquad \hat{\rho}'_\alpha = \frac{\rho'_\alpha}{\rho_\alpha}. \quad (8)$$

The first derivatives of η_α and ρ_α with respect to α such that $\phi_i = \frac{\sigma_i^2}{\sigma_i^2+\alpha}$, is given by:

$$\eta'_\alpha = 2\sum_{i=1}^{n}\left(\phi_i\frac{u_i^Tb}{\sigma_i}\right)\left(\frac{u_i^Tb}{\sigma_i}\phi'_i\right), \quad (9)$$

$$\rho'_\alpha = 2\sum_{i=1}^{n}((1-\phi_i)u_i^Tb)(u_i^Tb(1-\phi_i)'). \quad (10)$$

Then,

$$\begin{aligned}\phi'_i &= \frac{-\sigma_i^2}{(\sigma_i^2+\alpha)^2} = \frac{-\phi_i^2}{\sigma_i^2} = -\phi_i\left(\frac{\phi_i}{\sigma_i^2}\right)\\ &= -\phi_i\left(\frac{1}{\sigma_i^2+\alpha}\right) = \frac{-\phi_i}{\alpha}\left(\frac{\alpha}{\sigma_i^2+\alpha}\right)\\ &= \frac{-\phi_i}{\alpha}(1-\phi_i), \quad (11)\end{aligned}$$

$$(1-\phi_i)' = -\phi'_i = \frac{\phi_i}{\alpha}(1-\phi_i); \quad (12)$$

such that ϕ'_i is the first derivative of ϕ_i with respect to α. Then Eq.(9), Eq.(10) becomes as follows:

$$\eta'_\alpha = \frac{-2}{\alpha}\sum_{i=1}^{n}(1-\phi_i)\phi_i^2\frac{(u_i^Tb)^2}{\sigma_i^2}, \quad (13)$$

$$\rho'_\alpha = \frac{2}{\alpha}\sum_{i=1}^{n}(1-\phi_i)^2\phi_i(u_i^Tb)^2. \quad (14)$$

Then the relation between η'_α and ρ'_α is given by:

$$\begin{aligned}\rho'_\alpha &= -\frac{(1-\phi_i)\sigma_i^2}{\phi_i}\eta'_\alpha\\ &= -\frac{\sigma_i^2+\alpha}{\sigma_i^2}\left(1-\frac{\sigma_i^2}{\sigma_i^2+\alpha}\right)\sigma_i^2\eta'_\alpha\\ &= -(\sigma_i^2+\alpha)\left(\frac{\alpha}{\sigma_i^2+\alpha}\right)\eta'_\alpha\\ &= -\alpha\eta'_\alpha. \quad (15)\end{aligned}$$

The second derivatives of $\hat{\eta}_\alpha$ and $\hat{\rho}_\alpha$ with respect to α is given by:

$$\hat{\eta}''_\alpha = \frac{d}{d\alpha}\frac{\eta'_\alpha}{\eta_\alpha} = \frac{\eta''_\alpha\eta_\alpha - (\eta'_\alpha)^2}{\eta_\alpha^2}, \quad (16)$$

$$\hat{\rho}''_\alpha = \frac{d}{d\alpha}\frac{\rho'_\alpha}{\rho_\alpha} = \frac{\rho''_\alpha\rho_\alpha - (\rho'_\alpha)^2}{\rho_\alpha^2}. \quad (17)$$

From Eq.(15), we have

$$\rho''_\alpha = \frac{d}{d\alpha}(-\alpha\eta'_\alpha) = -\eta'_\alpha - \alpha\eta''_\alpha. \quad (18)$$

© 2015 NSP
Natural Sciences Publishing Cor.

Using Eqs.(8, 15, 16, 17 and 18), Then the curvature κ_α of the L-curve in Eq.(7) becomes as follows:

$$\begin{aligned}
\kappa_\alpha &= 2\frac{\left(\frac{\rho'_\alpha}{\rho_\alpha}\right)\left(\frac{\eta''_\alpha\eta_\alpha-(\eta'_\alpha)^2}{\eta_\alpha^2}\right)-\left(\frac{\rho''_\alpha\rho_\alpha-(\rho'_\alpha)^2}{\rho_\alpha^2}\right)\left(\frac{\eta'_\alpha}{\eta_\alpha}\right)}{\left(\frac{(\rho'_\alpha)^2}{\rho_\alpha^2}+\frac{(\eta'_\alpha)^2}{\eta_\alpha^2}\right)^{3/2}} \\
&= 2\frac{\left(\frac{-\alpha\eta'_\alpha}{\rho_\alpha}\right)\left(\frac{\eta''_\alpha\eta_\alpha-(\eta'_\alpha)^2}{\eta_\alpha^2}\right)-\left(\frac{(-\eta'_\alpha-\alpha\eta''_\alpha)\rho_\alpha-\alpha^2(\eta'_\alpha)^2}{\rho_\alpha^2}\right)\left(\frac{\eta'_\alpha}{\eta_\alpha}\right)}{\left(\frac{\alpha^2(\eta'_\alpha)^2}{\rho_\alpha^2}+\frac{(\eta'_\alpha)^2}{\eta_\alpha^2}\right)^{3/2}} \\
&= 2\frac{\left(\frac{-\alpha\eta\eta'_\alpha\eta''_\alpha+\alpha(\eta'_\alpha)^3}{\rho_\alpha\eta_\alpha^2}\right)-\left(\frac{-\rho(\eta'_\alpha)^2-\alpha\rho\eta'_\alpha\eta''_\alpha-\alpha^2(\eta'_\alpha)^3}{\rho_\alpha^2\eta_\alpha}\right)}{\left(\frac{\alpha^2\eta_\alpha^2(\eta'_\alpha)^2+\rho_\alpha^2(\eta'_\alpha)^2}{\rho_\alpha^2\eta_\alpha^2}\right)^{3/2}} \\
&= 2\frac{\left(\frac{\alpha\rho_\alpha(\eta'_\alpha)^3+\rho_\alpha\eta_\alpha(\eta'_\alpha)^2+\alpha^2\eta_\alpha(\eta'_\alpha)^3}{\rho_\alpha^2\eta_\alpha^2}\right)}{\frac{(\eta'_\alpha)^3(\alpha^2\eta_\alpha^2+\rho_\alpha^2)^{3/2}}{\rho_\alpha^3\eta_\alpha^3}} \\
&= 2\frac{\rho_\alpha\eta_\alpha}{\eta'_\alpha}\frac{\alpha\rho_\alpha\eta'_\alpha+\rho_\alpha\eta_\alpha+\alpha^2\eta_\alpha\eta'_\alpha}{(\alpha^2\eta_\alpha^2+\rho_\alpha^2)^{3/2}},
\end{aligned} \tag{19}$$

where the quantity η'_α is given by Eq.(13).

3 Generalized Cross Validation (GCV) Method

The GCV method is proposed by Gene H. Golub [5] used it as a parameter-choice method. It is a widely used and very successful predictive method for choosing the regularization parameter α ([6], [7], [8]). If an arbitrary element b_i of the left-hand side b of Eq.(1) is left out, then the corresponding regularized solution should predict this observation well, and the choice of regularization parameter α which minimizes the function $G(\alpha)$

$$G(\alpha) = \frac{\|Ax_\alpha - b\|_2^2}{(trace\,(I - AA_\alpha))^2}, \tag{20}$$

where $A_\alpha = (A^TA+\alpha I)^{-1}A^T$ is a matrix which produces the regularized solution x_α of Eq.(3) when multiplied with b, i.e., $x_\alpha = A_\alpha b$ and the *trace* of a matrix is the sum of its diagonal entries.

$$\|Ax_\alpha - b\|_2^2 = \sum_{i=1}^{n}((1-\phi_i)u_i^Tb)^2 = \sum_{i=1}^{n}\left(\left(\frac{\alpha}{\sigma_i^2+\alpha}\right)u_i^Tb\right)^2,$$
$$where \quad \phi_i = \frac{\sigma_i^2}{\sigma_i^2+\alpha}.$$

Also, from Eq.(4), we have

$$A_\alpha = (A^TA+\alpha I)^{-1}A^T = \sum_{i=1}^{n}\phi_i\frac{u_i^T}{\sigma_i}v_i,$$
$$A = \sum_{i=1}^{n}u_i\sigma_iv_i^T.$$

Then,

$$I - AA_\alpha = \sum_{i=1}^{n}(I-\phi_i) = \sum_{i=1}^{n}\left(\frac{\alpha}{\sigma_i^2+\alpha}\right),$$
$$(trace\,(I-AA_\alpha))^2 = \left(\sum_{i=1}^{n}\frac{\alpha}{\sigma_i^2+\alpha}\right)^2.$$

Using the singular value decomposition (SVD) of A, then the GCV function is given by:

$$G(\alpha) = \frac{\sum_{i=1}^{n}\left(\frac{u_i^Tb}{\sigma_i^2+\alpha}\right)^2}{\left(\sum_{i=1}^{n}\frac{1}{\sigma_i^2+\alpha}\right)^2}. \tag{21}$$

4 Dynamical Systems Method (DSM)

The DSM is proposed by A. G. Ramm ([19], [20], [21] and the references cited therein). It's based on an analysis of the solution of the Cauchy problem for linear and nonlinear differential equations in Hilbert space. Such an analysis was done for well-posed and ill-posed problems ([21] and the references sited therein). Consider a linear operator equation of the form:

$$F(x) = Ax - b = 0, \quad x \in H, \tag{22}$$

where H is a Hilbert space and A is a linear operator in H which is not necessarily bounded but closed and densely defined [11].

$$x'(t) = -x(t) + (T+a(t))^{-1}A^*b, \quad x(0) = x_0, \tag{23}$$

where $T := A^*A$, A^* is the transpose of A and $a(t) > 0$ is a nonincreasing function such that $a(t) \to 0$ as $t \to \infty$. The unique solution to Eq.(23) is given by

$$x(t) = x_0e^{-t} + e^{-t}\int_0^t e^s(T+a(s))^{-1}A^*\,b\,ds. \tag{24}$$

Eq.(24) leads to the following iterative formula [11] :

$$x_{n+1} = e^{-h_n}x_n + (1-e^{-h_n})(T+a_n)^{-1}A^*b_\delta, \; x_0 = 0, \tag{25}$$

where $h_n = t_{n+1} - t_n$, $h_n = q^n$, $1 \le q \le 2$, $\| b - b_\delta \| \le \delta$. using a relaxed discrepancy principle [19], Eq.(25) will terminate if x_n satisfies the following condition:

$$0.9\delta \le \| Ax_n - b_\delta \| \le 1.001\delta. \tag{26}$$

Also, as suggested in ([12], [11]) we can choose a_0 that satisfy the condition

$$\delta \le \phi(a_0) := \| Ax_{a_0} - b_\delta \| \le 2\delta, \tag{27}$$

by the following algorithm ([11], [22]) :

© 2015 NSP
Natural Sciences Publishing Cor.

1. As an initial guess for a_0 one takes $a_0 = \frac{\|A\|^2\delta_{rel}}{3}$, $\delta_{rel} = \frac{\delta}{\|b\|}$.
2. Compute $\phi(a_0)$. If it satisfies Eq.(27), then we are done. Otherwise, we go to step 3.
3. If $\frac{\phi(a_0)}{\delta} = c > 3$, then one takes $a_1 = \frac{a_0}{2(c-1)}$: as go back to step 2. If $2 < c \leq 3$ then one takes $a_1 = \frac{a_0}{3}$ and go back to step 2. Otherwise, we go to step 4.
4. If $\frac{\phi(a_0)}{\delta} = c < 1$, then $a_1 := 3a_0$. Otherwise we go to back to step 2.

5 Experiments Verifications

5.1 Example1

The image restoration test problem we use is taken from [2]. This test problem was developed at the US Air Force Phillips Laboratory, Lasers and Imaging Directorate, Kirtland Air Force Base, New Mexico. The original and degraded images are shown in Figure 1. This data has been widely used in the literature for testing image restoration methods. The observed blurred noisy images is computed by [13]:

$$b_\delta = b + \delta_{rel}\frac{\|b\|}{\|n\|}n, \tag{28}$$

where n is a matrix with random entries normally distributed with mean 0 and variance 1.

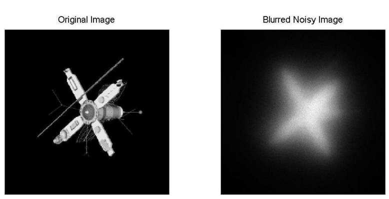

Fig. 1: Original and blurred noisy images.

To assess the performance of the different image restoration methods and to evaluate their comparative performance, two different standard performance indices have been used in this paper. They are namely Mean Squared Error (MSE) and Peak Signal to Noise Ratio (PSNR) and they are defined as follows:

$$MSE = \frac{1}{M \times N}\sum_{i=1}^{M}\sum_{j=1}^{N}|x(i,j) - \hat{x}(i,j)|^2, \tag{29}$$

$$PSNR(dB) = 10\log_{10}\left(\frac{255^2}{MSE}\right). \tag{30}$$

Where $x, \hat{x}$ represented the original and restored image having the same dimension $M \times N$ respectively, and dB represents the decibel unit. The higher the PSNR and lower the MSE in the restored image, the better is its quality. Moreover, human perception is the visual key indicator of improvement in quality for subjective comparisons of various restoration methods.

Figure 2, shows the results by the Tikhonov regularization method for blurred noisy image for different values of α, i.e., for α= 0.5, 0.05, 0.005 and 0.0005. Table 1, shows the results of MSE and PSNR in the restored images by the Tikhonov regularization method with different values of α. It is clear that the restored image which has high PSNR and lower MSE at α=0.005, is better than the restored images for other values of α. Consequently, it is obvious that a good choice for regularization parameter α is crucial to a successful image restoration.

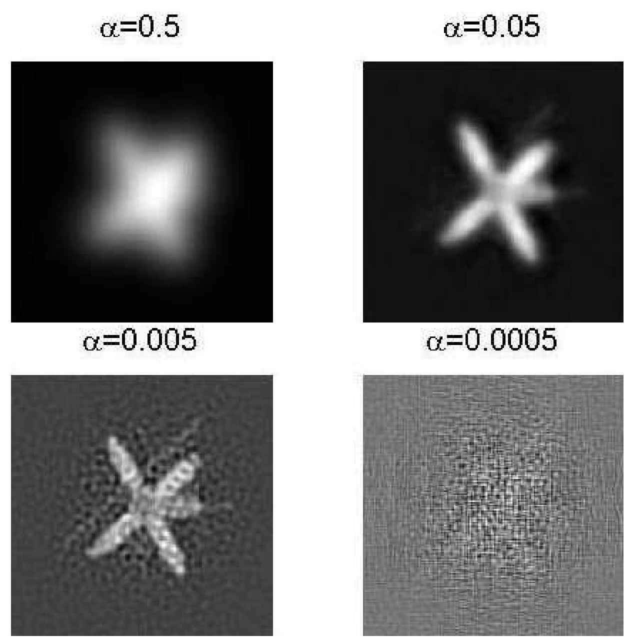

Fig. 2: Results obtained using Tikhonov regularization method with different values of α

Table 1: Results of MSE and PSNR for the restored images with different values of α

	α= 0.5	α= 0.05	α= 0.005	α= 0.0005
MSE	$1.5039e-009$	$5.6696e-010$	$5.4445e-010$	$7.5254e-008$
PSNR	136.3586	140.5953	140.7712	119.3655

Figure 3 and 4, show the optimum value of regularization parameter α, for blurred noisy image with $\delta_{rel} = 0.01$ using L-curve method and GCV method.

© 2015 NSP
Natural Sciences Publishing Cor.

From these figures, we observed that the optimum value of α using L-curve and GCV is 3.8533e-004 and 5.9308e-004 respectively.

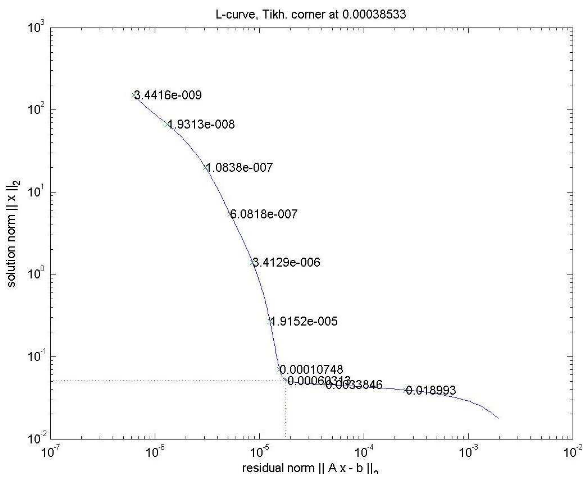

Fig. 3: L-curve method.

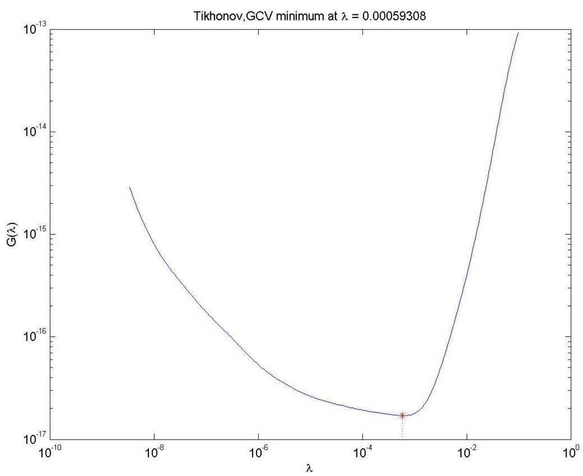

Fig. 4: GCV method.

Table 2, shows the results of MSE and PSNR in the restored images with different values of noise δ_{rel} = 0.01, 0.03 and 0.05 by Tikhonov regularization method and DSM where the regularization parameter obtained either by L-curve or GCV method for Tikhonov regularization method while it obtained by discrepancy principle for DSM.

Figure 5, 6 and 7, show the restored image by L-curve method, GCV method and DSM for different values of δ_{rel} at 0.01, 0.03 and 0.05 respectively.

Table 2: Results of MSE and PSNR for the restored images by Tikhonov regularization and DSM.

δ_{rel}= **0.01**			
	L-curve	**GCV**	**DSM**
MSE	$3.6691e-007$	$3.4426e-007$	$3.2115e-007$
PSNR	112.4852	112.7620	113.0637
δ_{rel}= **0.03**			
	L-curve	**GCV**	**DSM**
MSE	$9.4339e-007$	$8.7870e-007$	$7.7613e-007$
PSNR	108.3839	108.6924	109.2315
δ_{rel}= **0.05**			
	L-curve	**GCV**	**DSM**
MSE	$1.9511e-006$	$1.8202e-006$	$1.6422e-006$
PSNR	105.2279	105.5297	105.9765

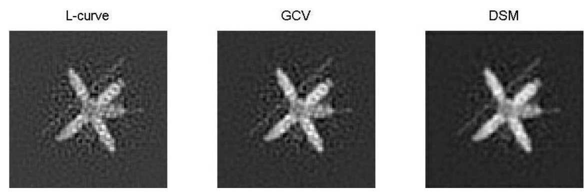

Fig. 5: δ_{rel}=0.01

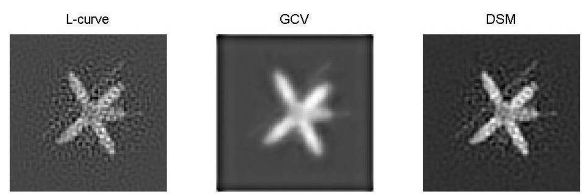

Fig. 6: δ_{rel}=0.03

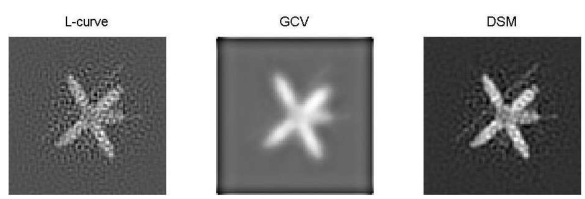

Fig. 7: δ_{rel}=0.05

5.2 Example2

In this example, we used the image restoration test problem taken from [2]. The original and degraded images are shown in Figure 8. The observed blurred noisy images is computed from Eq.(28) and use spatially invariant Gaussian blur is given by:

$$k(s,t) = \frac{1}{2\pi\sqrt{\gamma}} \exp\left\{ -\frac{1}{2} \begin{bmatrix} s & t \end{bmatrix} C^{-1} \begin{bmatrix} s \\ t \end{bmatrix} \right\}, \tag{31}$$

© 2015 NSP
Natural Sciences Publishing Cor.

where

$$C = \begin{bmatrix} \alpha_1^2 & \rho^2 \\ \rho^2 & \alpha_2^2 \end{bmatrix}, \quad \text{and} \quad \gamma = \alpha_1^2 \alpha_2^2 - \rho^4 > 0 \, .$$

The shape of the Gaussian blur depends on the parameters α_1, α_2 and ρ. In this test example $\alpha_1 = \alpha_2 = 4, \rho = 0$. Figure 9 and 10, show the optimum value of regularization parameter α, for blurred noisy image with $\delta_{rel} = 0.01$ using L-curve method and GCV method. From these figures, we observed that the optimum value of α using L-curve and GCV is 1.1730e-004 and 2.4028e-005 respectively.

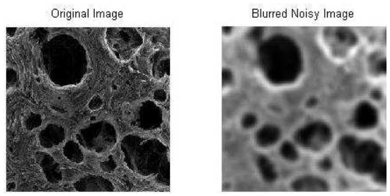

Fig. 8: Original and blurred noisy images.

Table 3, shows the results of MSE and PSNR in the restored images with different values of noise δ_{rel} = 0.01, 0.03 and 0.05 by Tikhonov regularization method and DSM.

Table 3: Results of MSE and PSNR for the restored images by Tikhonov regularization and DSM.

	δ_{rel}= 0.01		
	L-curve	**GCV**	**DSM**
MSE	$2.9179e-003$	$8.0155e-003$	$1.6422e-003$
PSNR	73.4801	69.0915	75.9765
	δ_{rel}= 0.03		
	L-curve	**GCV**	**DSM**
MSE	$1.3201e-002$	$1.3777e-002$	$2.2374e-003$
PSNR	66.9247	66.7393	74.6334
	δ_{rel}= 0.05		
	L-curve	**GCV**	**DSM**
MSE	$2.3250e-002$	$2.9175e-002$	$7.8764e-003$
PSNR	64.4666	63.4807	69.1675

Figure 11, 12 and 13, show the restored image by L-curve method, GCV method and DSM for different values of δ_{rel} at 0.01, 0.03 and 0.05 respectively.

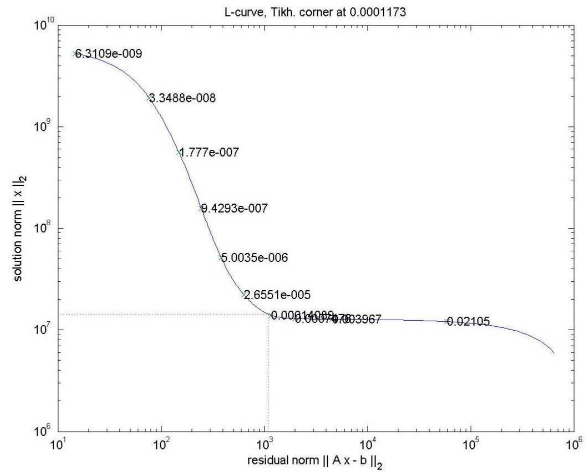

Fig. 9: L-curve method.

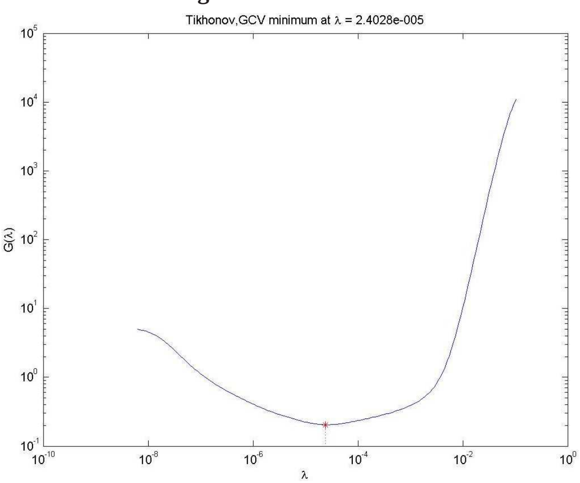

Fig. 10: GCV method.

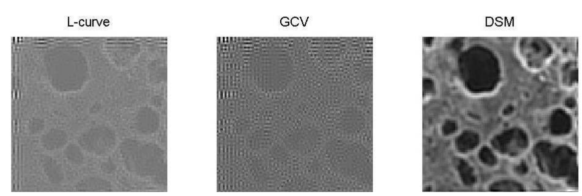

Fig. 11: δ_{rel}=0.01

6 Concluding Remarks

Image restoration is the process of removing blur and noise from degraded images to recover an approximation of the original image. The image degradation is usually modeled by a linear blur and an additive white noise process. The linear blur involved is always an ill-conditioned which makes image restoration problem an ill-posed problem for which the solutions are unstable. Procedures adopted to stabilize the inversion of ill-posed

© 2015 NSP
Natural Sciences Publishing Cor.

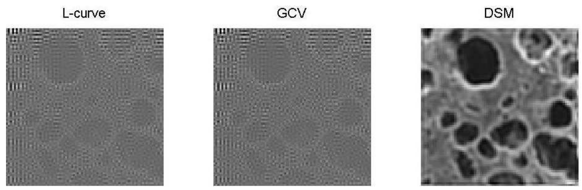

Fig. 12: δ_{rel}=0.03

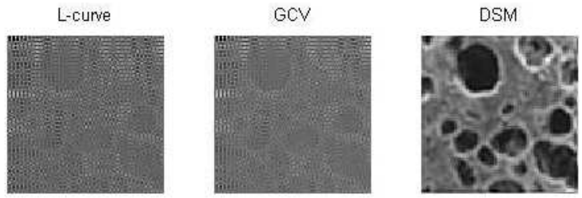

Fig. 13: δ_{rel}=0.05

problem are called regularization, so the selection of the regularization parameter is very important to the effect of image restoration. Dynamical systems method (DSM), Tikhonov regularization method, L-curve method and generalized cross validation (GCV) are presented for solving this ill-posed problems. From comparative studies and the numerical results it is clear that DSM showed improved restored images compared to L-curve and GCV.

References

[1] M. Banham and A. Katsaggelos, Digital Image Restoration, *IEEE Signal Processing Magazine*, 2(14), (1997), 24-41.
[2] S. Berisha and J. Nagy, Iterative Methods for Image Restoration, *Academic Press Library in Signal Processing: Image, Video Processing and Analysis, Hardware, Audio, Acoustic and Speech Processing*, 4, (2013), 193.
[3] A. Carasso, Linear and Nonlinear Image Deblurring: A Documented Study,*SIAM Journal on Numerical Analysis*, 6(36), (1999), 1659-1689.
[4] J. Chung, Filtering Methods for Image Restoration, *PhD diss., Honors Thesis, Department of Mathematics and Computer Science, Emory University*, (2004).
[5] G. Golub, M. Heath and G. Wahba, Generalized Cross-Validation as a Method for Choosing a Good Ridge Parameter, *Technometrics*, 2(21), (1979), 215-223.
[6] G. Golub and U. Matt, Generalized Cross-Validation for Large Scale Problems, *Journal of Computational and Graphical Statistics*, 1(6), (1997), 1-34.
[7] P. Hansen , Rank-Deficient and Discreat Ill-Posed Problems: Numerical Aspects of Linear Inversion, *Siam, Philadelphia, PA*, (1998).
[8] P. Hansen, Regularization Tools: A Matlab Package for Analysis and Solution of Discrete Ill-Posed Problems, *Numerical Algorithms*, 1(6), (1994), 1-35.
[9] P. Hansen, The L-curve and Its Use in the Numerical Treatment of Inverse Problems, Invited Chapter in P. Johnston (Ed.), *Computational Inverse Problems in Electrocardiology, WIT Press, Southampton*, (2001), 119-142.
[10] P. Hansen and D. O'Leary, The Use of the L-curve in the Regularization of Discrete Ill-Posed Problems, *Siam Journal on Scientific Computing*, 6(14), (1993), 1487-1503.
[11] N. Hoang and A. Ramm, Solving Ill-Conditioned Linear Algebraic Systems by the Dynamical Systems Method (DSM), *Inverse Problems in Science and Engineering*, 5(16), (2008), 617-630.
[12] N. Hoang and A. Ramm, Dynamical Systems Method for Solving Linear Finite-Rank Operator Equations, *Ann. Polon. Math*, 95, (2009), 77-93.
[13] N. Hoang and A. Ramm, Dynamical Systems Gradient Method for Solving Ill-Conditioned Linear Algebraic Systems, *Acta Applicandae Mathematicae*, 2(111), (2010), 189-204.
[14] S. Jayaraman, S. Esakkirajan and T. Veerakumar, Digital Image Processing, *Tata McGraw-Hill Education*, (2011).
[15] C. Lawson and R. Hanson, Solving Least Squares Problems, *Prentice-Hall, Englewood Cliffs, NJ*, (1974).
[16] D. Mackenzie, Novel Imaging Systems Rely on Focus-Free Optics, *Siam News*, 6(36), (2003).
[17] E. Meinel, Origins of Linear and Nonlinear Recursive Restoration Algorithms, *Journal of the Optical Society America A*, 6(3), (1986), 787-799.
[18] N. Nguyen, P. Milanfar and G. Golub, Efficient Generalized Cross Validation with Applications to Parametric Image Restoration and Resolution Enhancement, *IEEE Transactions on Image Processing*, 9(10), (2001), 1299-1308.
[19] A. Ramm, A New Discrepancy Principle, *Journal of Mathematical Analysis and Applications*, 1(310), (2005), 342-345.
[20] A. Ramm, Dynamical Systems Method for Solving Operator Equations, *Communications in Nonlinear Science and Numerical Simulation*, 4(9), (2004), 383-402.
[21] A. Ramm, Inverse Problems, *Springer, New York*, (2005).
[22] N. Sweilam, A. Nagy and M. Alnasr, An Efficient Dynamical Systems Method for Solving Singularly Perturbed Integral Equations with Noise, *Computers and Mathematics with Applications*, 7(58), (2009), 1418-1424.
[23] A. Tikhonov, Regularization of Incorrectly Posed Problems, *Soviet Math. Doklady*, 4, (1963), 1624-1627.
[24] A. Tikhonov and V. Arsenin, Solutions of Ill-Posed Problems, *Winston, Washington, D. C.*, (1977).
[25] J. Zhang and Q. Wang, An Iterative Conjugate Gradient Regularization Method for Image Restoration, *Journal of Information and Computing Science*, 1(5), (2010), 055-062.

© 2015 NSP
Natural Sciences Publishing Cor.

Nasser H. Sweilam, professor of numerical analysis at the Department of Mathematics, Faculty of Science, Cairo University. He was a channel system Ph.D. student between Cairo University, Egypt, and TU-Munich, Germany. He received his Ph.D. in Optimal Control of Variational Inequalities, the Dam Problem. He is the Head of the Department of Mathematics, Faculty of Science, Cairo University, since May 2012. He is referee and editor of several international journals, in the frame of pure and applied Mathematics. His main research interests are numerical analysis, optimal control of differential equations, fractional and variable order calculus, bio-informatics and cluster computing and ill-posed problems.

A. M. Nagy, doctor of numerical analysis at Department of Mathematics, Faculty of Science, Benha University. He received his M.Sc. in Numerical Analysis from Benha University in 2007, and his Ph.D. in Numerical Analysis from Universitá Degli Studi Di Bari Aldo Moro, Italy in 2012. He is referee of several international journals, in the frame of pure and applied Mathematics. His main research interests are Numerical solutions of ill-posed problems, Numerical solutions of ordinary differential equations (IVPs and BVPs), Volterra integro-differential equations (VIDEs), Numerical solutions of partial differential equations (PDEs), and Numerical solutions of fractional differential equations (FDEs).

Tamer Farag received the B.S. And M.S. degrees in Computational Science from Cairo University, Egypt, in 1998 and 2002, respectively. He received his Ph.D. From Graduate school of natural science and technology, Okayama University Japan. He joined the Department of Mathematics, Faculty of Science, Cairo University in December 1997 as assistant, lecture and become an assistant Prof. at December 2010. He was a visitor researcher at Okayama University from Oct 2009 to Oct 2010 and from Nov 2013 to Nov 2014. His research interests include wireless network, image processing and combinatorial optimization application. He is a member of IEEE and ACM.

Amira. S. Abo-Elyazed, teaching assistant of Computational Science at the Department of Mathematics, Faculty of Science, Cairo University, Egypt. She received the B.S. degree in Mathematics and Computational Science from Department of Mathematics, Faculty of Science, Cairo University, Egypt, in 2007. She received the Pre-Master degree in Computational Science from Department of Mathematics, Faculty of Science, Cairo University, Egypt, in 2011. Her main research interests are Numerical solutions of ill-posed problems and image processing.

© 2015 NSP
Natural Sciences Publishing Cor.